*Optica Applicata, Vol. XIV, No. 1, 1984*

# Correlation of optical and generation properties of YAG: $Nd^{3+}$ rods*

JERZY CZESZKO, SŁAWOMIR KACZMAREK

Institute of Quantum Electronics, Military Technical Academy, 01-489 Warszawa-Bemowo, Poland.

## 1. Introduction

Optical investigations of the quality of YAG: $Nd^{3+}$' laser rods with the system of Twyman-Green interferometer do not give complete information as to their application into laser systems, especially in selection of the dye Q-switch.

This work presents the results of optical investigations of YAG: $Nd^{3+}$ rods performed for 145 Polish rods of 3 mm diameter and 50 mm length. These investigations included the Twyman-Green interferometric measurements and determination of the features of a multimode generation for the giant pulse generation.

## *2.* Interferometric investigations

The investigations were made to verify the optical quality of YAG: $Nd^{3+}$ single crystals, from which the laser rods were cut off. Typical interferograms of YAG single crystals and photographs with light passing across are presented in photos (Figs. 1-3).

Rods were cut off from the regions of equal distribution of interference fringes of the same direction and density. The quality of mechanical working was measured in the system of Mach-Zehnder interferometer, where the mutual. parallelism of rod ends and their flatness were measured. The rods with the parallelism less than 5" and the flatness greater than $\lambda/20$ were omitted. The optical quality of YAG rods were determined from the number of interference fringes on the unit length of rod in the system of Twyman-Green interferometer.

The results of optical quality measurements for some of the rods investigat-ed are presented in Table l. Typical interferograms of YAG rods are presented in photographs (Figs. 4-6).

---

*This paper has been presented at the European Optical Conference (EOC'83), May 30-June 4, 1983, in Rydzyna, Poland.

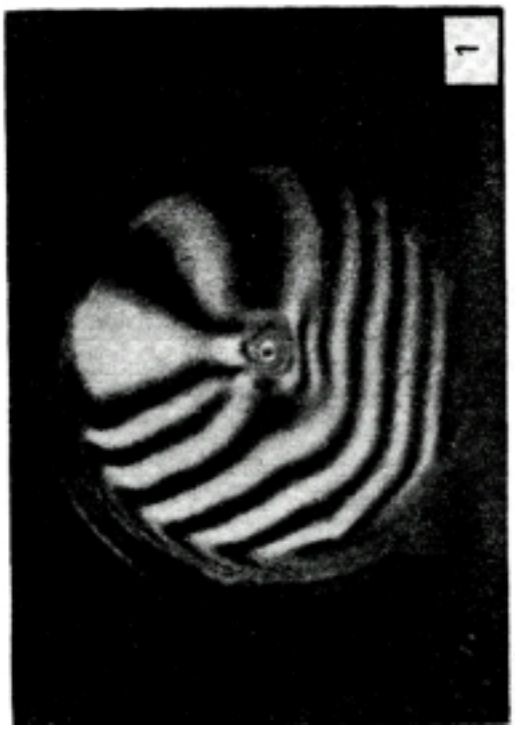

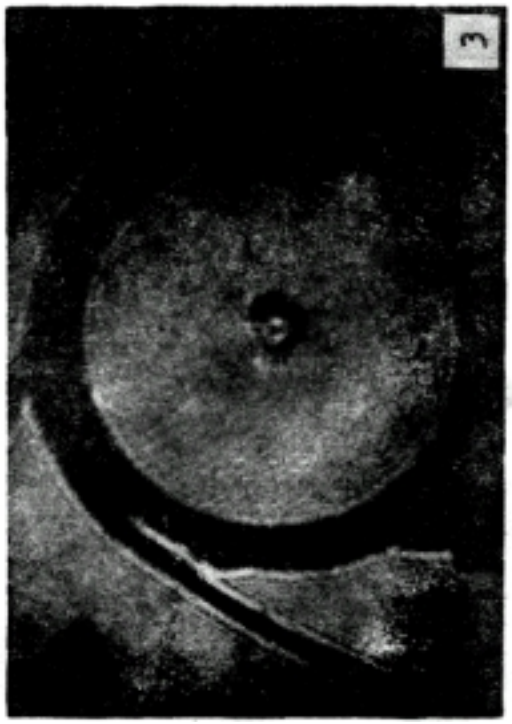

Fig. 1. The interferogram of YAG single crystal for zeroth background of interferometer

Fig. 2. The interferogram of YAG single crystal for compressed background of interferometer

Fig. 3. The image of YAG single crystal with light passing across the crystal

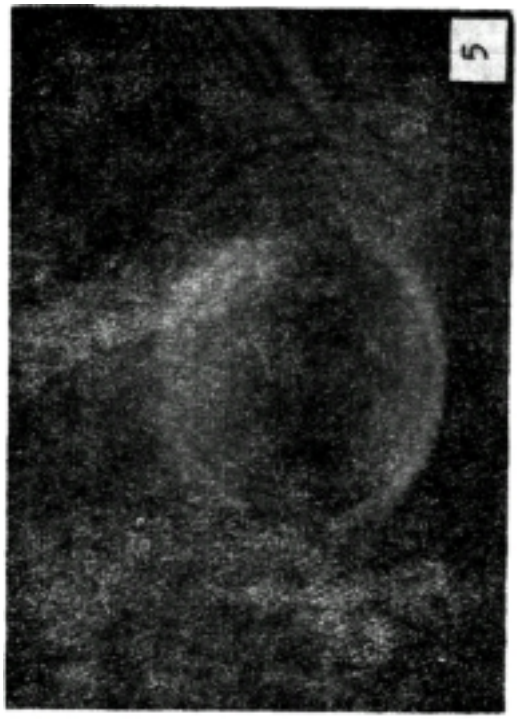



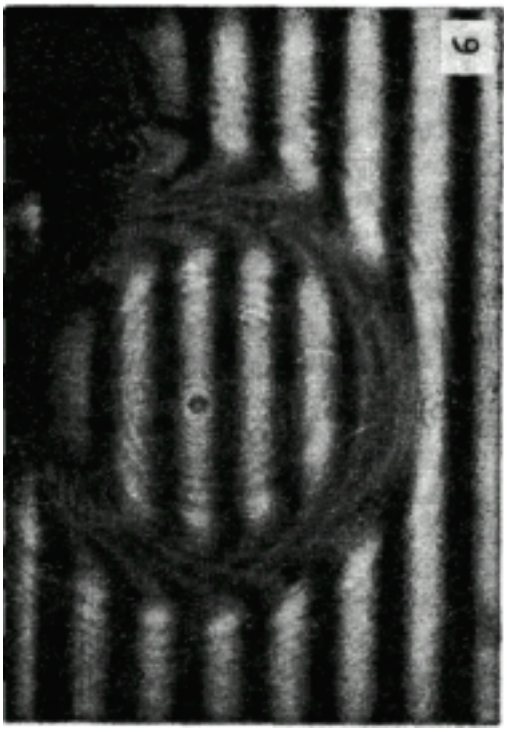


**Fig. 4.** The interferogram of YAG: $Nd^{3+}$ rod for the zeroth background of interferometer with zero-order fringes on the object

**Fig. 5.** The interferogram of YAG: $Nd^{3+}$ rod for the zeroth background of interferometer with the one fringe on the object

**Fig. 6.** The interferogram of YAF: $Nd^{3+}$ rod for the compressed background of interferometer (6-th order of interference) which shows the quality of optical working

Table 1

| No. of a rod | 17 | 63 | 65 | 82 | 86 | 87 | 88 | 89 | 90 | 91 | 92 | 93 | 97 | 98 | 99 |
|---|---|---|---|---|---|---|---|---|---|---|---|---|---|---|---|
| No. of fringes on the unit length | 0 | 0.2 | 0 | 0.4 | 0.2 | 0.4 | 0 | 0.1 | 0 | 0.2 | 0 | 0.2 | 0.4 | 0.4 | 0.2 |
| No. of a rod | 101 | 102 | 103 | 104 | 105 | 106 | 107 | 108 | 123 | 124 | 126 | 131 | 135 | 141 | 81 |
| No. of fringes on the unit length | 0.4 | 0 | 0.2 | 0.4 | 0 | 0.4 | 0.2 | 0.2 | 0.2 | 0.4 | 0.4 | 0.4 | 0.2 | 0.4 | 0.8 |
| No. of a rod | 80 | 79 | 78 | 77 | 72 | 100 | | | | | | | | | |
| No. of fringes on the unit length | 0.2 | 0.4 | 0.4 | 0.4 | 0.4 | 0.5 | | | | | | | | | |

## 3. The measurement of absorption coefficient

The absorption coefficient ($\rho$) was determined for some output mirrors by dynamical measurement of rod parameters at the beginning of generation [1]. The transmissions of these mirrors were: 11°/o, 15°/o, 48°/o, 60.9°/o and 69°/o.

The relationship between the absorption coefficient ($\rho$) and the coefficient of laser amplification ($k$) is the following [1]:

$$k = \rho - \frac{1}{l}\ln T_f - \frac{1}{2l}\ln R_1 R_2 \tag{1}$$

where: $l$ — active length of laser rod,

$T_f$—transmission of plastic foil nonlinear absorber for a neodymium laser,

$R$ — reflection coefficient of mirrors.

The absorption coefficient can be found from a ratio of the pumping energy $E_p$ to output energy while the threshold energy of generation is to be found as indicated in the following formula [1]:

$$\frac{E_p}{E_{th}} = 1 - \frac{1}{2\rho l}\ln R. \tag{2}$$

From the dependence of $E_p$ on ln $R$ we can calculate the absorption coefficient $\rho$, for YAG: $Nd^{3+}$ rod. The dependence of threshold energy on the exit losses is as follows [1]:

$$(E_p - E_{th}) = k_r \tan\alpha, \tag{3}$$

$$k_r = \frac{1}{2l}\ln\frac{1}{R_1 R_2}. \tag{4}$$

For the mirrors applied here we have:

$$k_{r_1}(R_2 = 0.889) = \frac{1}{8.6cm}\ln\frac{1}{0.999\times 0.889} = 0.014\,cm^{-1},$$

$$k_{r_2}(R_2 = 0.845) = \frac{1}{8.6\,cm}\ln\frac{1}{0.999\times 0.845} = 0.019\,cm^{-1},$$

$$k_{r_3}(R_2 = 0.52) = \frac{1}{8.6\,cm}\ln\frac{1}{0.999\times 0.52} = 0.076\,cm^{-1},$$

$$k_{r_4}(R_2 = 0.391) = \frac{1}{8.6\,cm}\ln\frac{1}{0.999\times 0.391} = 0.109\,cm^{-1},$$

$$k_{r_5}(R_2 = 0.302) = \frac{1}{8.6\,cm}\ln\frac{1}{0.999\times 0.302} = 0.139\,cm^{-1}.$$

Let us examine the measurement of $\rho$, say for instance for rod of number 126. Table 2 contains the results of output energy measurements for this rod for a different pumping energy and output mirror transmission.

Table 2

| $E_p$[J] | $E_{out}$ [mJ] $T_z$ = 11% | $E_{out}$ [mJ] $T_z$ = 48% | $E_{out}$ [mJ] $T_z$ = 60.9% | $E_{out}$ [mJ] $T_z$ = 69% | Up [V] |
|---|---|---|---|---|---|
| 2.02 | 1.67 | - | - | - | 600 |
| 2.37 | 3.11 | 1.67 | - | - | 650 |
| 2.75 | 4.23 | 4.52 | 1.13 | - | 700 |
| 3.15 | 5.09 | 6.78 | 2.83 | 1.41 | 750 |
| 3.59 | 6.78 | 9.89 | 5.64 | 3.96 | 800 |
| 4.05 | 8.47 | 13.56 | 8.76 | 7.06 | 850 |
| 4.54 | 9.61 | 17.23 | 12.71 | 10.17 | 900 |
| 5.06 | 11.30 | 21.75 | 16.67 | 15.54 | 950 |

A plot of $E_p = f_2(E_{out})$ is a straight line. The value of $E_{th}$ for the individual transmissions *is* found by the least squares method (Table 3).

Table 3

| $T_z$ | 11% | 48% | 60.9% | 69% |
|---|---|---|---|---|
| $E_{th}$ [J] | 1.45 | 2.15 | 2.7 | 3.02 |
| $k_r$ [cm$^{-1}$] | 0.014 | 0.076 | 0.109 | 0.139 |

A plot of $E_{th} = f_1(E_{out})$ is a straight line too, and its slope gives the value of $\rho$. Applying also the least squares method, we have $\rho = 0.092$. In this way we have measured the values of absorption coefficient $\rho$ for 145 Polish rods. It has been noticed that among the rods investigated there are such for which the value of $E_{mult\ gen}$ does not depend on the angle of rod rotation with respect to optical axis, for example, for the rod No. 130, and such rods which demonstrate this dependence, for example, rod No. 115.

Hence, for the next measurements the angle of rod rotation has been optimized with regard to the maximal energy of multimode generation.

## 4. Estimation of the quality of the Q-switch elements

To the bleachable dye Q-switch we applied the plastic foil nonlinear absorber for a neodymium laser (FNA 1064), which was stuck into two parallel flat plates from the BK-7 glass. Transmission mirror was put on one plate and antireflection layer on the other one. The dye, applied here, is optically and chemically resistant. We have obtained the time of giant pulse Q-switching equal to 7-8 ns. The FNA stands about 40,000 pulses (the details concerning the dye and FNA will be presented in the work by Konarski [2]). The technology of production of the Q-switch requires the ideal purity conditions.

The parameter which characterizes the FNA and mirror is their transmissions for $\lambda = 1.064$.

We have prepared FNA with 25-55°/o transmission and mirrors with 45-79%. The Q-switch parameters, their selection into YAG: $Nd^{3+}$ rods, generation properties for some rods are shown in Table 4.

## 5. Selection of the Q-switch into the rod

It is necessary to examine the influence of FNA transmission, $T_f$ mirror transmission, $T_z$ and resultant transmission, $T_w$, on the obtained energetic characteristics of lasers heads. The following characteristics have been determined: $E_{th}$ of giant pulse generation vs. $T_w$ (Fig 7), $E_{out}$ of giant pulse generation vs. $T_w$

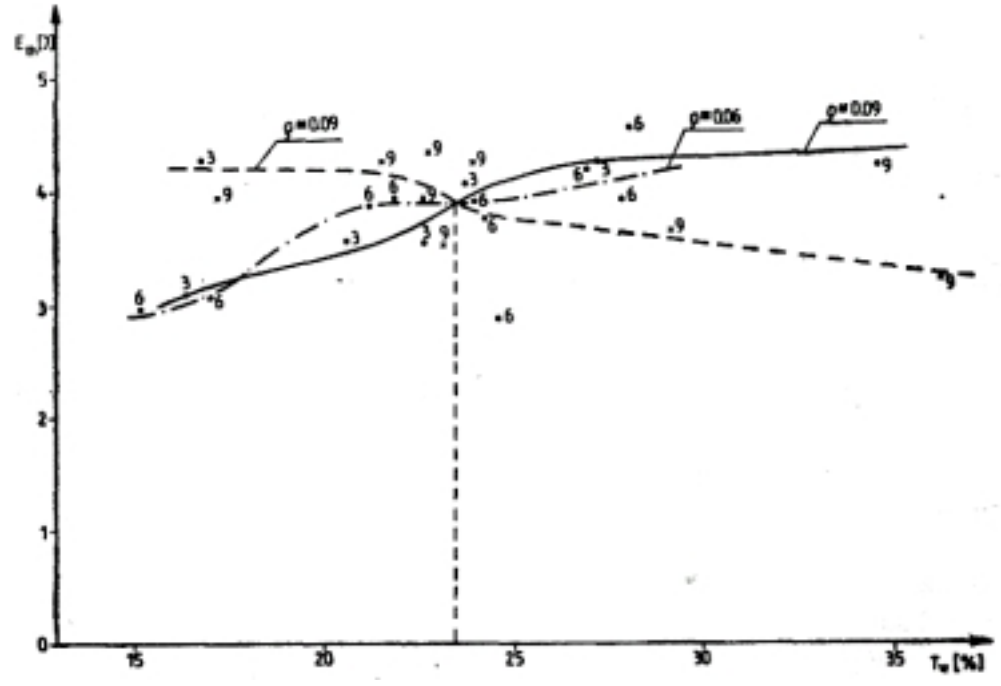


Pig. 7. The dependence of threshold pumping energy $E_{th}$ on the resultant transmission

**Table 4**

| No. | No. of a rod | $T_z$[%] | $T_f$[%] | $T_w$[%] | $U_1$ [V]–$U_2$ [V] ($E_1$ [J]–$E_2$ [J]) | $\Delta U$ [V] | $E_{out}$[mJ] | $\varrho$ | Number of interference fringes on the unit length |
|---|---|---|---|---|---|---|---|---|---|
| 1 | 2 | 3 | 4 | 5 | 6 | 7 | 8 | 9 | 10 |
| 1 | 17 | 61.2 | 37 | 24.3 | 870–1000 (4.24–5.61) | 130 | 6.8 | 0.003 | 0 |
| 2 | 63 | 63 | 47 | 21.6 | 870–990 (4.24–5.49) | 120 | 4.2 | 0.088 | 0.1 |
| 3 | 65 | 65 | 47 | 34.6 | 870–960 (4.24–5.16) | 90 | 5.0 | 0.021 | 0 |
| 4 | 82 | 55 | 50 | 21.9 | 840–1000 (3.95–5.61) | 160 | 7.0 | 0.062 | 0.2 |
| 5 | 86 | 63 | 42 | 20.6 | 800–915 (3.58–4.69) | 115 | 4.6 | 0.024 | 0.1 |
| 6 | 87 | 59.6 | 37 | 21.2 | 830–885 (3.86–4.39) | 55 | 4.6 | 0.063 | 0.2 |
| 7 | 88 | 63 | 40.6 | 22.7 | 800–890 (3.58–4.44) | 90 | 7.7 | 0.031 | 0 |
| 8 | 89 | 61.2 | 37 | 24.3 | 820–910 (3.77–4.64) | 90 | 4.6 | 0.065 | 0.05 |
| 9 | 90 | 63 | 37 | 24.7 | 720–850 (2.9–4.05) | 130 | 5.0 | 0.057 | 0 |
| 10 | 91 | 60.5 | 37 | 24.2 | 750–865 (3.15–4.19) | 115 | 5.0 | 0.040 | 0.1 |
| 11 | 92 | 60 | 39.5 | 24.0 | 840–940 (3.95–4.95) | 100 | 4.4 | 0.056 | 0 |
| 12 | 93 | 58.6 | 37 | 23.8 | 855–910 (4.09–4.64) | 55 | 5.6 | 0.038 | 0.1 |
| 13 | 97 | 61 | 39.5 | 24.2 | 760–860 (3.24–4.14) | 100 | 4.5 | 0.049 | 0.2 |

| 1 | 2 | 3 | 4 | 5 | 6 | 7 | 8 | 9 | 10 |
|---|---|---|---|---|---|---|---|---|---|
| 14 | 98 | 72 | 50 | 36.3 | 760–860 (3.24–4.14) | 100 | 4.5 | 0.092 | 0.2 |
| 15 | 99 | 63 | 40.6 | 22.7 | 730–825 (2.98–4.79) | 95 | 4.2 | 0.053 | 0.1 |
| 16 | 101 | 69 | 39.7 | 29.2 | 810–910 (3.67–4.64) | 100 | 5.6 | 0,078 | 0.2 |
| 17 | 102 | 61.5 | 40.6 | 16.4 | 740–830 (3.07–3)86) | 90 | 5.1 | 0.022 | 0 |
| 18 | 103 | 69 | 39 | 23.2 | 780–870 (3.41–4.24) | 90 | 7.7 | 0.092 | 0.1 |
| 19 | 104 | 69 | 39 | 15.2 | 730–820 (2.98–3.77) | 90 | 4.5 | 0.056 | 0.2 |
| 20 | 105 | 55 | 40.5 | 17.0 | 740–860 (3.07–4.14) | 120 | 4.2 | 0.065 | 0 |
| 21 | 106 | 63 | 40.6 | 20.8 | 820–925 (3.77–4.79) | 105 | 4.8 | 0.045 | 0.2 |
| 22 | 107 | 69 | 43.2 | 29.3 | 800–890 (3.58–4.44) | 90 | 4.5 | 0.046 | 0.1 |
| 23 | 108 | 69 | 39 | 27.8 | 840–955 (3.95–5.10) | 115 | 4.0 | 0.059 | 0.1 |
| 24 | 123 | 55 | 40.5 | 16.8 | 880–1000 (4.34–5.61) | 120 | 8.5 | 0.030 | 0.1 |
| 25 | 124 | 44 | 39 | 17.3 | 840–1000 (3.95–5.61) | 160 | 7.0 | 0.117 | 0.2 |
| 26 | 126 | 55 | 50 | 22.8 | 880–1000 (4.34–5.61) | 120 | 6.7 | 0.098 | 0.2 |
| 27 | 131 | 59.2 | 37 | 24.0 | 870–980 (4.24–5.38) | 110 | 7.0 | 0.096 | 0.2 |
| 28 | 135 | 55 | 50 | 22.7 | 840–980 (3.95–5.38) | 140 | 7.9 | 0.099 | 0.1 |
| 29 | 141 | 61 | 50 | 27.2 | 870–1000 (4.24–5.61) | 130 | 5.0 | 0.037 | 0.2 |

| | | | | | | | | | |
|---|---|---|---|---|---|---|---|---|---|
| 03 | 81 | 52 | 50 | 26.2 | 880–1000 (4.34–5.01) | 120 | 4.9 | 0.040 | 0.4 |
| 31 | 80 | 52 | 50 | 26.2 | 840–990 (3.95–5.49) | 150 | 6.4 | 0.044 | 0.1 |
| 32 | 79 | 47 | 45.5 | 21.6 | 875–1000 (4.29–5.61) | 125 | 5.2 | 0.079 | 0.2 |
| 33 | 78 | 55 | 50 | 28.1 | 890–1000 (4.44–5.61) | 110 | 5.0 | 0.058 | 0.2 |
| 34 | 77 | 52 | 37 | 19.8 | 875–1000 (4.29–5.61) | 125 | 6.8 | 0.041 | 0.2 |
| 35 | 72 | 61 | 43.8 | 27.0 | 870–950 (4.24–5.06) | 80 | 5.1 | 0.062 | 0.2 |
| 36 | 100 | 69 | 47 | 32.4 | 830–920 (3.86–4.74) | 90 | 5.7 | 0.323 | 0.25 |

(Fig. 8), $E_{th}$ of giant pulse generation vs. $T_f$ (Fig. 9), the area width of giant pulse generation, $\Delta U$, vs. $T_f$ and $E_{mult\ gen}$ of multimode generation vs. $T_s$.

Figure 7 shows the dependence of threshold pumping energy, $E_{th}$, on the resultant transmission. For this purpose the results shown in Table 4 for different values of absorption coefficient $\rho$ ($\rho \approx 0.03$, 0.06, and 0.09) have been

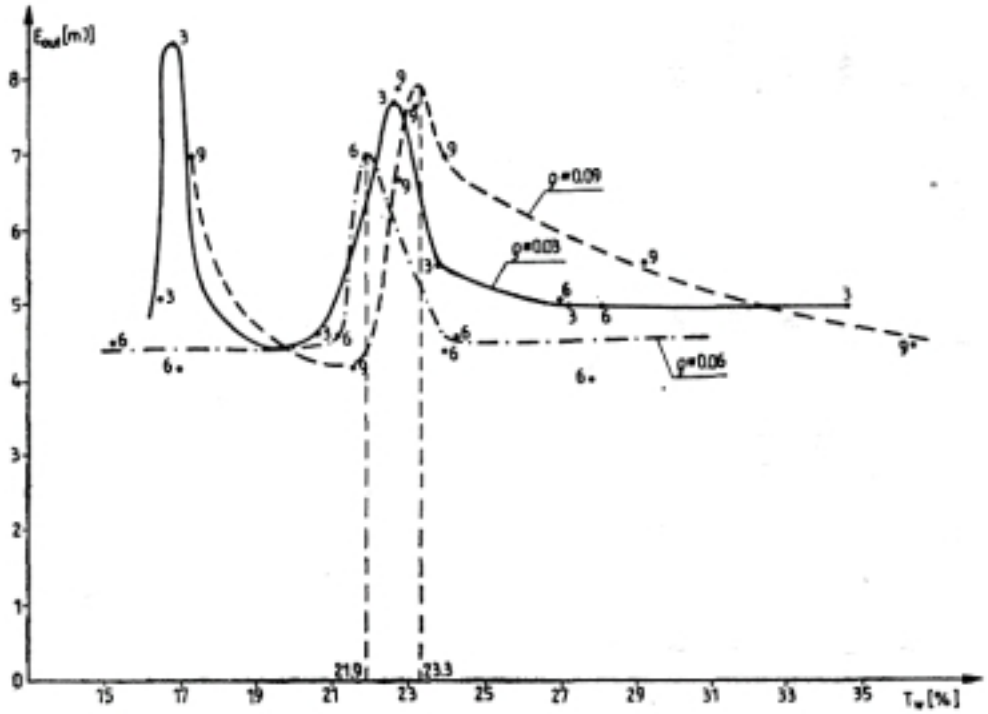


Pig. 8. The dependence of giant pulse energy generation $E_{out}$ on the resultant transmission for rods with different values of $\rho$

selected and presented in Table 5. From this Table and plots shown in Fig. 7 it follows that $E_{th}$ of giant pulse generation depends monotonically on the change of $T_w$ for an arbitrary $\rho$. For the rods of r ≈ 0.03 and 0.06 it is observed that the threshold energy grows with $T_w$ but for the rods with $\rho \approx 0.09$ this energy decreases with the increasing $T_w$. The characteristic point is located at the place of the curves intersection (23.5°/o $T_w$).

Figure 8 presents the dependence of giant pulse energy generation, $E_{out}$ on the resultant transmission for rods with different values of $\rho$. There are two maximum areas of the generating energy, for $T_w$ = 17°/o and 23°/o, which are independent of the $\rho$ value.

The dependence of the threshold generation voltage for giant pulse generation on the transmission of FNA for an arbitrary transmissions of mirrors is shown